JOURNAL OF MATERIALS SCIENCE 25 (1990) 2481–2486

Rapidly solidified Si–Fe alloys

M. A. CUNHA*, G. W. JOHNSON‡
*Cia. Aços Especiais Itabira - ACESITA, Núcleo de Desenvolvimento Tecnológico, Av. Afonso Pena 4000, Belo Horizonte MG, Brazil
‡School of Materials, Division of Metallurgy, The University of Leeds, Leeds, UK

Si–Fe ribbons produced by the chill-block melt-spinning method, with silicon contents of 5.59 and 6.06 wt%, were annealed at temperatures between 1000 and 1215° C, in vacuum, 5.33 to 13.13 Pa. During annealing for 1 h abnormal grain growth was observed to occur, with modification of the as-cast texture. Two main texture components were identified: a(1 0 0)[0 *k l*] texture as the main texture component at all temperatures; and the (4 2 1)[−5 8 4] or a combination of (4 2 1) [−5 8 4] and (3 2 1)[−5 6 3] as the second component. The growth of the two main components is affected by the annealing temperature and the annealing time.

d.c. coercivity and core loss are significantly reduced by annealing with minimum values being obtained for a 6.06 wt% Si ribbon annealed at 1085° C for 1 h.

1. Introduction

Silicon–iron alloys with silicon content around 6.5 wt % offer a great potential for core loss reduction in electrical machinery, due to the high resistivity, low anisotropy and low magnetostriction of the alloy [1].

The silicon content of commercial silicon–iron sheets, however, has been limited to a maximum of around 3.5 wt % Si, due to the poor ductility of the higher silicon alloys [1].

Recently, rapid solidification methods have been used to produce high silicon–iron ribbons directly from the melt [2, 5]. The product is a microcrystalline ribbon of improved ductility, that can be bent and cold rolled.

The structure and the magnetic properties of as-cast and as-annealed Si–Fe ribbons have been reported by a number of authors [2–13]. Tsuya *et al.* [3] and Arai *et al.* [6, 7] reported the affect of the annealing conditions on the texture and the magnetic properties. Very low core loss has been reported [8] for high silicon–iron ribbons with sharp cube texture (1 0 0)[0 *k l*].

This paper presents the results of an investigation of the affects of the annealing conditions on the microstructure, texture and magnetic properties of high silicon–iron ribbons produced by the chill-block melt-spinning method.

2. Experimental methods

The ribbons used in this work were prepared by the chill-block melt-spinning method [14]. The apparatus used and the production of the ribbons are described elsewhere [15].

The alloys were prepared from electrolytic iron (99.95 wt %) and metallic silicon (98.96 wt %) by induction melting in an alumina crucible. The ribbons were cast in air, on a mild steel wheel of 200 mm diameter, and showed clean, silver-coloured surfaces. The silicon content of the master alloys and the dimensions of the ribbons used in this investigation are given in Table I.

Annealing treatments were carried out at different temperatures in the range of 1000° to 1215° C, in vacuum (5.33 to 13.13 Pa). The average heating rate was 8.25° C min^{-1}. Specimens for heat treatment were straight pieces of ribbon about 160 mm long and 1 m long pieces of ribbon wound into toroids of 24 mm diameter.

The microstructure of the ribbons was observed by optical microscopy on a longitudinal section and on a section parallel to the ribbon surface. The grain boundaries were revealed by etching the polished surface in 5% nital for 15 to 20 sec.

The texture was examined by X-ray diffraction, using CrKα radiation, and by the observation of etch pits on the surface of the grains.

d.c. coercivity and power loss were measured for as-cast and as-annealed specimens. Coercivity was measured from the hysteresis loop, recorded by the hysteresigraph method [16]. An integrating fluxmeter and an *XY* recorder were used to record the hysteresis loop at a frequency of 0.2 Hz and maximum field of 1690 A m^{-1}. Specimens were straight pieces of ribbon 160 mm long.

Power loss was measured at 50 and 60 Hz using a system similar to that developed by Blundell *et al.* [17], under conditions of sinusoidal induction. Specimens were toroids 24 mm in diameter and 1.2 mm^2 cross-section, containing three copper wire windings: a 50 turn field coil, a 50 turn feedback coil and a five turn search coil.

TABLE I Master alloy silicon content and ribbon dimensions

Sample	Silicon (wt %)	Thickness (μm)	Width (mm)
A	5.59	37.5	3.5
B	6.06	54.0	4.5

0022–2461/90 $03.00 + .12

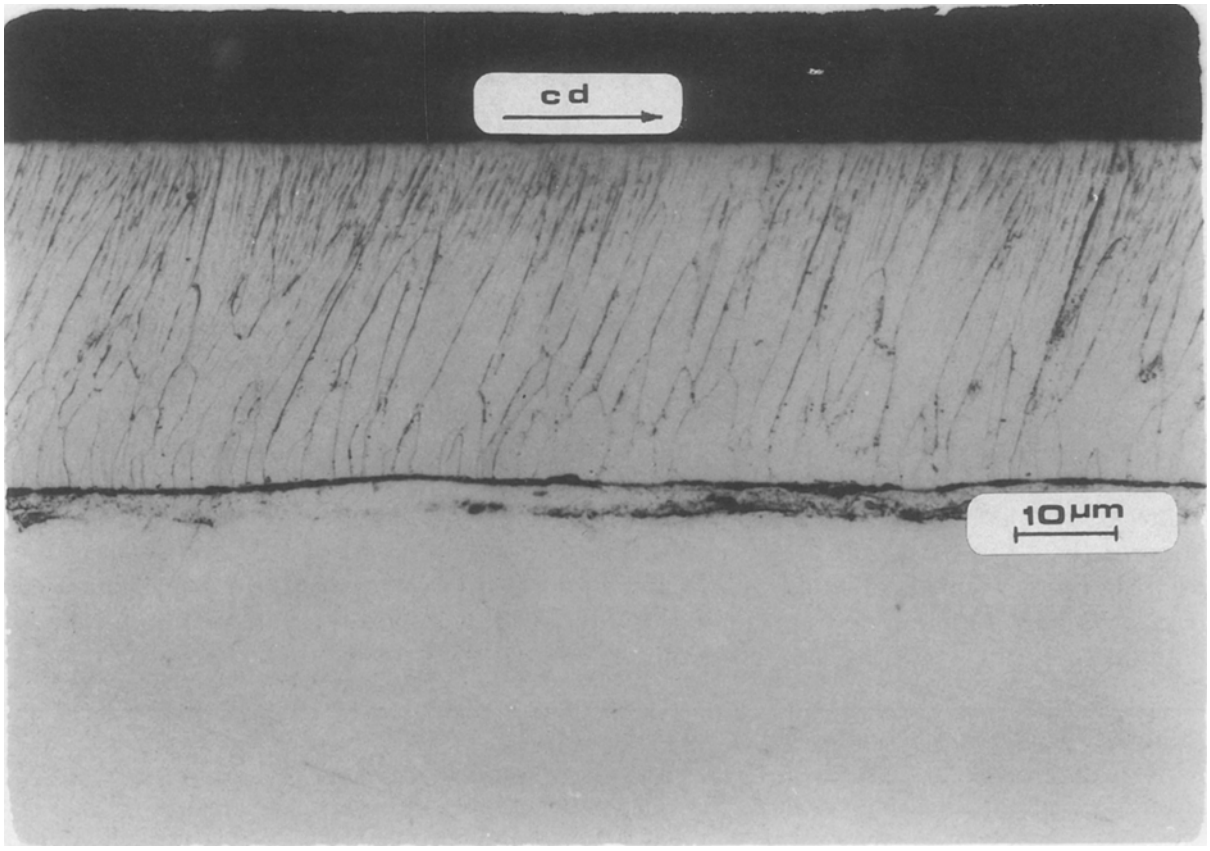

Figure 1 Micrograph taken on a longitudinal section.

3. Results

3.1. Microstructure

The microstructure of melt-spun Si–Fe ribbons cast on a steel substrate consists of a chill crystal zone adjacent to the interface of the wheel (bottom surface), that develops into elongated columnar dendritic grains and extends across the whole section to the free surface (top surface), as shown in the micrograph in Fig. 1. The columnar grains lean towards the leading end of the ribbon (casting direction c.d.) at an angle of approximately 20° with the ribbon normal.

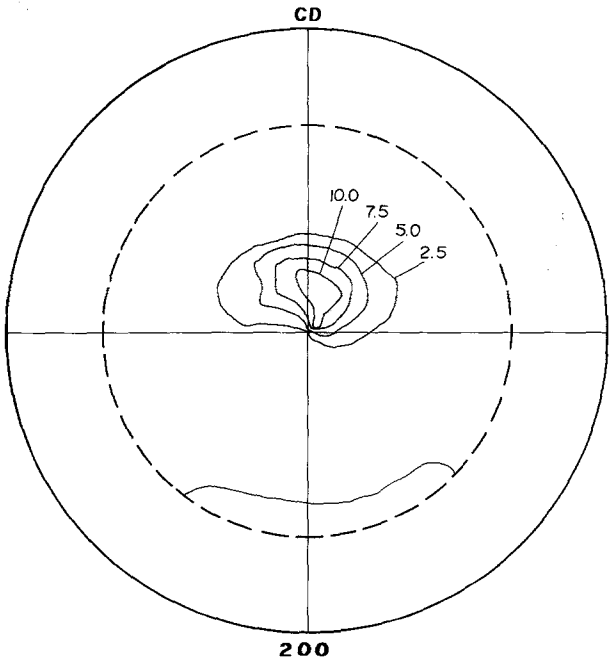

Figure 2 (2 0 0) pole figure, top surface of the as-cast ribbon.

The texture is consistent with the observed microstructure, revealing no preferred orientation at the bottom surface and a [0 0 1] fibre texture on the top surface, with the fibre axis tilted 20° towards the casting direction, as illustrated by the (2 0 0) pole figure in Fig. 2.

The microstructure observed on a section parallel to the ribbon surface consists of small equiaxed grains, of average grain size less than 10 μm. After annealing for 1 h at temperatures between 1000 and 1215° C secondary recrystallization is observed to occur. Fig. 3 shows the percentage of secondary recrystallization plotted against the annealing temperature for samples A and B. The average grain size for the secondary grains

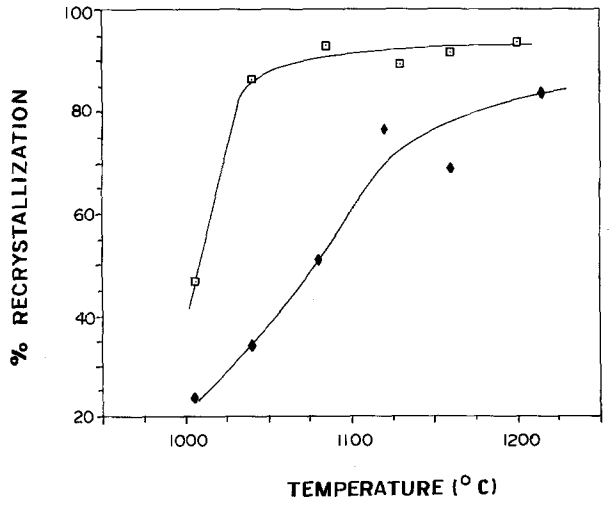

Figure 3 Surface area fraction of secondary grains (□ sample A. ◆ sample B).

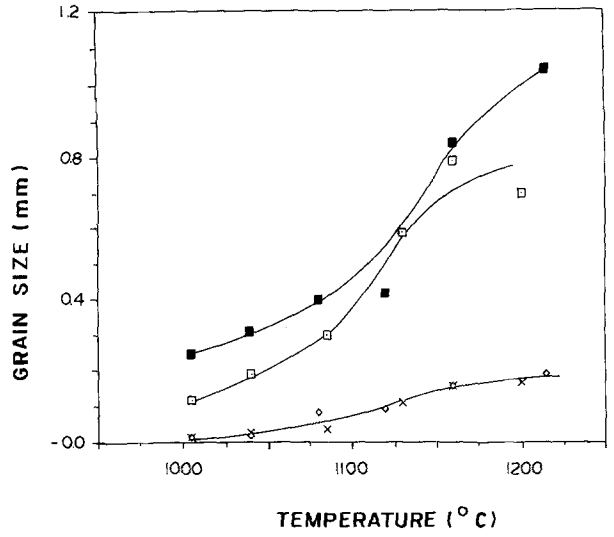

Figure 4 Averaged grain size plotted against the annealing temperature (□ A secondary, x A primary, ■ B secondary, ◇ B primary).

and for the unconsumed primary grains are shown in Fig. 4.

For sample A the surface area fraction occupied by the secondary grains increases with the annealing temperature and reaches a plateau at 1040° C, with more than 90% of the surface area occupied by the secondary grains. A similar tendency is observed for sample B, with the surface area fraction tending to a plateau at around 1120° C and approximately 73% secondary recrystallization.

3.2. Texture

The orientation of the secondary grains in samples A and B was similar. Two main components were identified: a (1 0 0)[0 k l] texture as the main component, at all annealing temperatures, and a second texture component, characterized by a rotation of around 30° or more from the ideal cube texture and a certain degree of alignment in the plane of the specimen, described as (4 2 1)[− 5 8 4] or a combination of (4 2 1)[− 5 8 4] and (3 2 1)[− 5 6 3], that rotates approximately ± 65° around the direction normal to the specimen plane. (2 0 0) and (1 1 0) pole figures for a specimen of sample A, annealed at 1215° C for 1 h, are shown in Fig. 5. The relative intensity of the different components of the texture was estimated by integrating the X-ray data for the (2 0 0) reflection. The results are expressed by the ratio between the integrated intensity within intervals of 5° (I_θ) and the total integrated intensity (I_t). The ratio is proportional to the density of (1 0 0) planes within an angle θ and θ minus 5 degrees (θ − 5) from the specimen surface. Fig. 6a shows the ratio I_θ/I_t plotted against the annealing temperature. It shows that increasing the annealing temperature weakens the (1 0 0)[0 k l] component of the texture and strengthens the second component, (4 2 1)[− 5 8 4] and (3 2 1)[− 5 6 3].

To investigate the effect of the annealing time on the texture, specimens of sample A were annealed at 1100° C for different annealing times, up to 160 min. In this experiment the average heating rate was approximately 48° C min^{-1}. The results are shown in Fig. 6b. It shows that the intensity of the (1 0 0)[0 k l] component of the texture decreases with the annealing time and the intensity of the second component increases with the annealing time. Short annealing times and lower annealing temperatures favour the growth of the (1 0 0)[0 k l] component.

3.3. Magnetic properties

Coercivity plotted against annealing temperature is shown in Fig. 7. The coercivity of the as-cast specimen is also shown in the figure.

There is a significant reduction of the coercivity after annealing, specially for sample A. Coercivity is observed to go down with the annealing temperature, reach a minimum value and rise slightly for the higher annealing temperatures. The minimum coercivity, for sample A, was approximately 48 A m^{-1}, obtained at

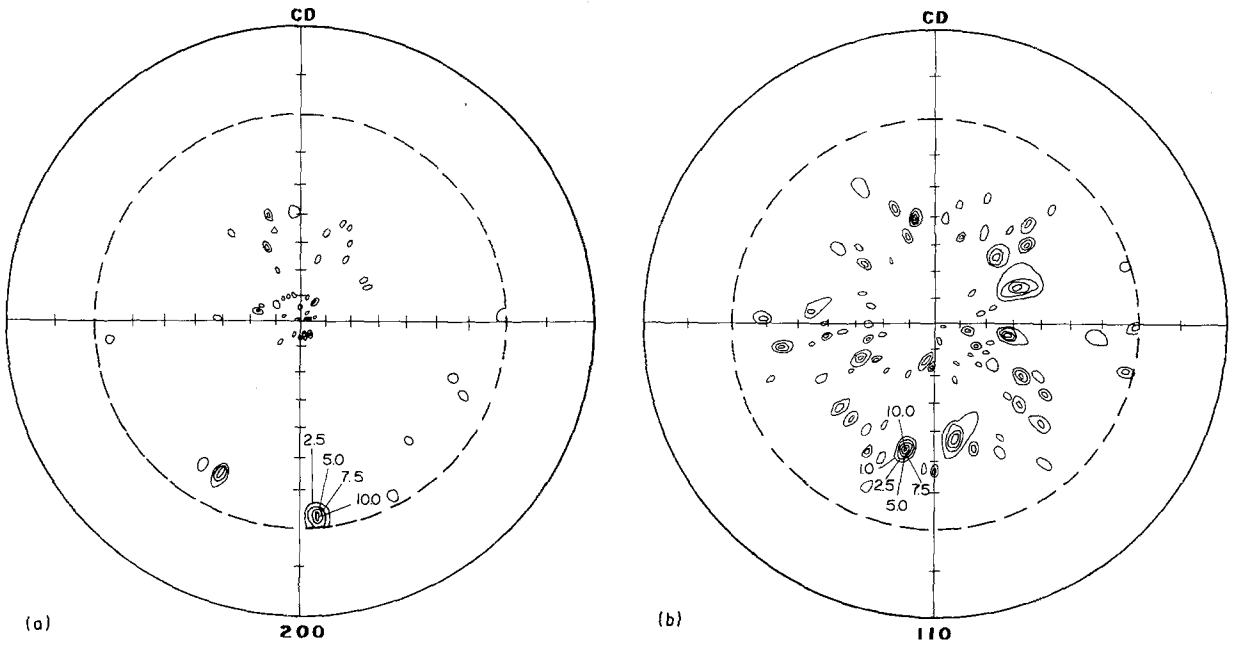

Figure 5 (a) (2 0 0) pole figure, specimen A, annealed at 1215° C for 1 h; (b) (1 1 0) pole figure, specimen A, annealed at 1215° C for 1 h.

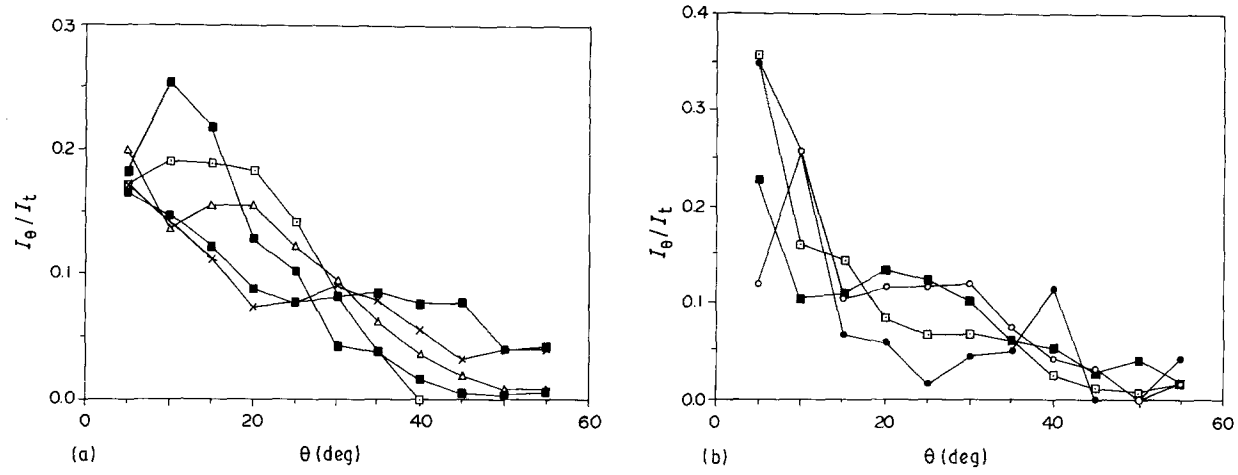

Figure 6 (a) I_θ/It plotted against θ as a function of the (a) annealing temperature (⊡ as-cast, △ 1005° C, ■ 1040° C, x 1130° C, ■ 1215° C) and (b) annealing time (□ 15 min, ● 31 min, ■ 63 min, ○ 160 min).

around 1040 to 1100° C. The lowest individual value was 32.5 A m^{-1}, obtained at 1040° C. For sample B the minimum coercivity was 24 A m^{-1}, at around 1080 to 1120° C, and the lowest individual measurement was 20 A m^{-1}, at 1085° C.

Core loss values for sample B, measured at 50 and 60 Hz, are shown in Fig. 8 as a function of the magnetic induction. Core loss was significantly reduced by annealing the specimens. The lowest core loss values were obtained at 1085 to 1160° C. The minimum core loss values, at 50 Hz, were around 0.30 and 0.20 W kg^{-1} at test inductions of 1.0 and 0.8 T, respectively.

4. Discussion

4.1. Microstructure and texture

Annealing the ribbons in the range of 1000 to 1215° C for 1 h, in vacuum, resulted in abnormal grain growth, or secondary recrystallization, with some modification of the original texture.

In this process some grains, with diameter a few times larger than the average grain diameter, grow rapidly, consuming the smaller matrix grains. Surface energy differences between grains of different orientations is believed to control the selection of the grains which are to grow. Grains having the lowest surface energy tend to grow and cover the ribbon surface during annealing [18, 19].

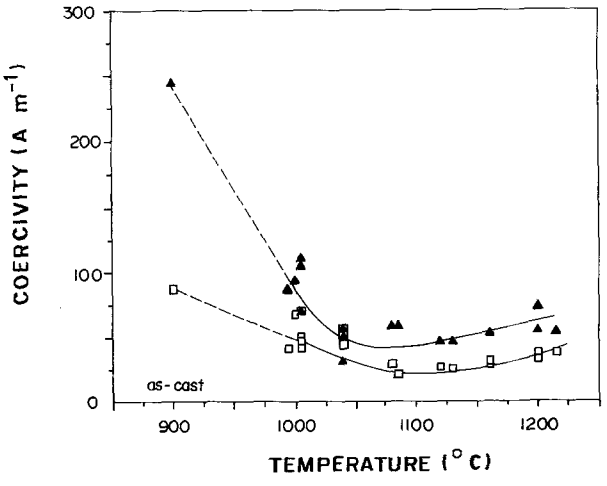

Figure 7 Coercivity plotted against annealing temperature for samples A (▲) and B (□).

The hierarchy of surface energy can be altered by impurity atoms adsorbed on the surface. Adsorption of oxygen [20] is known to favour the reduction of the energy of the (1 0 0) oriented surfaces. Tsuya *et al.* [3] and Arai *et al.* [6, 7] investigated the effect of the vacuum pressure and the annealing temperature on grain growth in high silicon–iron ribbons. According to their results, the (1 0 0) plane would have the lowest surface energy between 1000 and 1200° C, for vacuum pressure in the range of 5.3 and 13.3 Pa, as used in the present experiments. Above around 1200° C, (1 1 0) planes would tend to have the lowest surface energy.

The results shown in the previous section are similar to those reported by Tsuya *et al.* [3] and Arai *et al.* [6, 7], in the sense that the main component of the texture is of the (1 0 0)[0 k l] type. A second component of the texture, identified in this work, (4 2 1)[−5 8 4] or (4 2 1)[−5 8 4] and (3 2 1)[−5 6 3], tends to form. The growth of the second component is favoured by higher temperature and prolonged annealing.

The hierarchy of the surface energy may change during annealing, due to changes in the surface condition. Reduction of the oxide layer and/or segregation of solute atoms to the surface are factors that can contribute to change the surface energy hierarchy during annealing. Increasing the annealing temperature may cause the changes to take place earlier in the process, so altering the relative intensity of the different texture components.

Secondary recrystallization was not complete, particularly in sample B. It has been suggested [15] that the oxide layer present in the surface of the as-cast ribbon may have contributed to retard the progress of secondary recrystallization, and may also have contributed to the difference in the extent of secondary recrystallization between the two samples.

4.2. Magnetic properties

A significant reduction of coercivity and core loss follows the partial replacement of the original structure of small cross-section columnar grains by the structure of large secondary grains, where the main texture component is a (1 0 0)[0 k l] cube texture. The

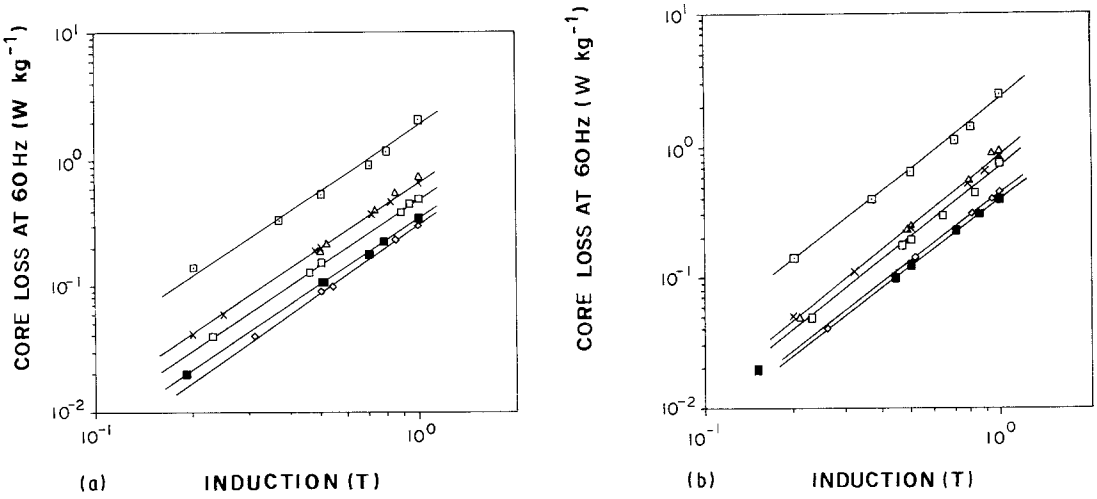

Figure 8 (a) Core loss plotted against induction at (a) 50 Hz and (b) 60 Hz. (□ as-cast, △ 1015° C, x 1040° C, ◇ 1085° C, ■ 1160° C, □ 1200° C).

minimum in the coercivity coincides with the beginning of the plateau in the percentage of secondary recrystallization curves.

After the plateau is reached two factors contribute to shape the coercivity against temperature curve: the average grain size increases with the annealing temperature, and the second component of the texture grows in intensity with the annealing temperature.

The second texture component contributes to reduce the density of easy direction of magnetization, [0 0 1], in the plane of the specimen. The two factors act in opposite directions, resulting in a somewhat flat minimum in the coercivity curves. Coercivity rises slightly at higher temperatures, coinciding with the maximum intensity of the second texture component (Fig. 6a) and the downward curvature in the average grain size curves, in Fig. 4.

The core loss data in Fig. 8 show that core loss varies similarly to the coercivity with the annealing temperature. The lowest core loss values were obtained in the range 1085 to 1160° C.

In Table II the minimum coercivity and core loss (50 Hz) values, obtained at 1085° C, are compared with minimum values obtained from references [4] and [13]. There is a discrepancy between the coercivity values reported in the literature by different authors. As noted by Tenwick *et al.* [13], the discrepancy may result from differences in the measuring techniques used. The minimum core loss obtained in this work is slightly higher than that reported in reference [4]. The higher silicon content of the latter may have contributed for the difference observed. Tsuya *et al.* [4] have also reported to have obtained complete secondary recrystallization and a (1 0 0)[0 k l] texture. The loss measurements in this work were made using the test equipment of Tenwick *et al.* [13] who obtained a significantly higher core loss value. A (1 0 0)[0 k l] texture was also reported, but the extent of secondary recrystallization in their samples was not given, which may account for the higher core loss.

TABLE II Minimum coercivity and core loss values (50 Hz)

Reference	H_c (Am^{-1})	$P_{1T/50\,Hz}$ (W kg^{-1})
This work	20	0.30
[4]–6.5 wt % Si	4	0.22
[13]–6.5 wt % Si	19	0.64

5. Conclusions

Abnormal grain growth, or secondary recrystallization, resulted from annealing the Si–Fe ribbons in vacuum, 5.33 to 13.13 Pa, at temperatures between 1000 and 1215° C.

The orientation of the secondary grains was characterized by two main texture components: a (1 0 0)[0 k l] orientation as the main component of the texture and a second component, described as (4 2 1)[− 5 8 4] or a combination of (4 2 1)[− 5 8 4] and (3 2 1)[− 5 6 3].

The partial replacement of the original as-cast structure of small cross-section columnar grains by the structure of large secondary grains, where the main texture was a (1 0 0)[0 k l] cube texture, resulted in a significant reduction of coercivity and core loss after annealing. Lower annealing temperature and shorter annealing time favoured the growth of the cube texture, whereas higher annealing temperature and longer annealing time favoured the growth of the second component.

Acknowledgements

This research received the financial support from the Conselho Nacional de Desenvolvimento Cientifico e Tecnologico, CNPq (Brazil), through a grant conceded to one of the authors (MAC). The authors are grateful to Dr H. A. Davies, School of Materials, University of Sheffield, for the use of equipment for measuring core loss.

References

1. R. M. BOZORTH, in "Ferromagnetism". (Van Nostrand, Amsterdam, 1951) p. 570.
2. N. TSUYA and K. I. ARAI, *Jpn. J. Appl. Phys.* **18** (1979) 207–208.
3. N. TSUYA, K. I. ARAI, K. OHMORI, H. SHIMANAKA and T. KAN, *IEEE Trans. Magn.* **MAG16** (1980) 728–733.
4. N. TSUYA and K. I. ARAI, in "Recent Magnetics for Electronics", edited by Y. Sakúrai, JARECT **10** (1983). 245–255.

5. C. F. CHANG, R. L. BYE, V. LAXMANAN and S. K. DAS, *IEEE Trans, Magn.*, **MAG20** (1984) 553–558.
6. K. I. ARAI, N. TSUYA and K. OHMORI, *ibid.* **MAG17** (1981) 3154–3156.
7. K. I. ARAI, H. TSUMITAKE and K. OHMORI, *ibid.* **MAG20** (1984), 1463–1465.
8. K. I. ARAI, K. OHMORI, *Metall. Trans* **17A** (1986) 1295–1299.
9. M. ENOKIZONO, N. TESHIMA and N. NARITA, *IEEE Trans. Magn.* **MAG18** (1982) 1007–1013.
10. K. NARITA, M. ENOKIZONO, N. TESHIMA and Y. MORI, *J. Magn. Magn. Mater.* **19** (1980) 143–144.
11. K. NARITA, N. TESHIMA, Y. YAMASHIRO, Y. J. SHIN and Y. YOSHIDA, *ibid.* **41** (1984) 86–92.
12. M. J. TENWICK and H. A. DAVIES, *Int. J. Rap. Solid.* **1** (1985) 143–155.
13. *Idem.*, in Proceedings Fifth International Conference Rapidly Quenched Metals", edited by S. Steeb and H. Warlimont (Elsevier, North Holland, 1985) pp. 1, 67–70.
14. H. H. LIEBERMANN and C. D. GRAHAM Jr., *IEEE Trans. Magn.* **MAG12** (1976) 921–923.
15. M. A. CUNHA, Ph.D Thesis, Leeds University, Leeds (1988).
16. B. D. CULLITY, in "Introduction to Magnetic Materials" (Addison-Wesley, Reading, Ma, 1972) p. 666.
17. M. G. BLUNDELL, K. J. OVERSHOTT and C. D. GRAHAM, *J. Magn. Magn. Mater.*, **19** (1980) 243–244.
18. K. FOSTER, J. J. KRAMER and G. W. WEINER, *Trans. Metall. Soc. AIME* **227** (1963) 185–188.
19. J. L. WALTER and C. G. DUNN, *Trans. Metall. Soc. AIME* **218** (1960) 914–922.
20. *Idem.*, *Acta. Metall.* **8** (1960) 497–503.

Received 9 February
and accepted 24 August 1989